Fuel Cells

DOI: 10.1002/anie.201104498

Molecular Catalysis in a Fuel Cell**

*Takahiro Matsumoto, Kyoungmok Kim, and Seiji Ogo**

Molecular hydrogen is considered to be the most promising of chemical fuels in terms of removing our dependence on fossil fuels, but the development of cheap, efficient, fuel-cell systems has not yet been realized. Currently, fuel cells are based on the heterogeneous, homolytic splitting of H_2 on a platinum surface, but these fuel cells have the obvious problem that Pt is both scarce and expensive.[1] Furthermore, few improvements in efficiency have been achieved in over a hundred years, so a new model for fuel-cell catalysis is required to generate a fuel-cell-based economy. Though a few related systems have been reported,[2–4] the successful construction of a new type of fuel cell has not been achieved to date.

Fuel-cell development can be taken in an entirely new direction by the introduction of molecular catalysts capable of working in homogeneous solutions. Molecular catalysts have the advantage of being highly variable in terms of design, and solution-phase catalysis is important because it enables us to directly observe the details of the mechanism (Figure 1).[5] By combining these two features, we can view the path to greater efficiency.

This laboratory has previously reported just such a catalyst and, as a result of its solution-phase behavior, we were able to determine the action of this catalyst in precise detail.[6] The catalyst is based on a biologically inspired $Ni^{II}Ru^{II}$ aqua complex, $[Ni^{II}LRu^{II}(H_2O)(\eta^6\text{-}C_6Me_6)](NO_3)_2$ ($[\mathbf{1}](NO_3)_2$, L = *N*,*N*′-dimethyl-*N*,*N*′-bis(2-mercaptoethyl)-1,3-propanediamine; Scheme 1) and is a functional model of natural [NiFe]hydrogenases. It is soluble in water, and aqueous-phase reactions showed that it was able to catalyze the oxidation of H_2 to protons. Importantly, the catalyst functioned by means of a mechanism new to chemistry, involving two molecules of H_2 in one cycle and a remarkable, low-valent, $Ni^{I}Ru^{I}$ active center. This cycle also proceeded via an unusually stable hydride complex $[Ni^{II}(H_2O)L(\mu\text{-}H)Ru^{II}(\eta^6\text{-}C_6Me_6)](NO_3)$ ($[\mathbf{2}](NO_3)$), which was so stable

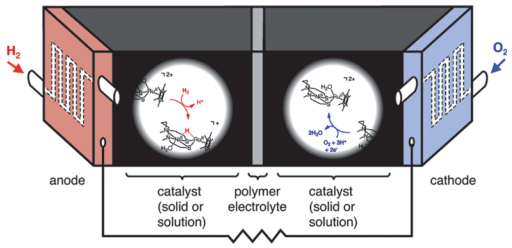

Figure 1. Direct observation of catalysts in a fuel cell[5]—an abstract depiction of a fuel cell. Water-saturated H_2 and O_2 gases flow through conduits in the electrodes (red and blue). In solution-phase experiments, water-soluble catalysts with the NO_3^- counteranion are dissolved in the gas conduits. In solid-phase experiments, water-insoluble catalysts with the $CF_3SO_3^-$ counteranion are immobilized on carbon cloth sandwiched between the electrodes and the proton-conducting polymer electrolyte. Protons pass through the polymer electrolyte and electrons flow through an electrical circuit to the cathode.

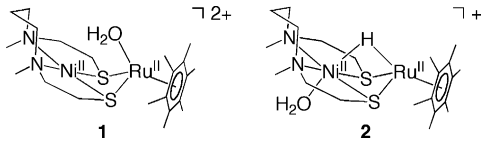

Scheme 1. Molecular catalysts **1** and **2**.

that it was more convenient to use **2** as the starting point for experiments, and hence the experimental descriptions below refer to **2** rather than **1**. In a major development for this chemistry, we have now been able to apply **2** to the catalysis of the complementary reduction, that is, O_2 to H_2O. In other words, **2** is capable of catalyzing both the oxidation of H_2 and the reduction of O_2 in the formation of H_2O. This ability to promote both sides of the process has not been observed for any kind of molecular catalyst to date.

We are thus able to report the performance of a functioning molecular fuel cell with $Ni^{II}Ru^{II}$ hydride complex **2** as the catalyst for both the anode and the cathode. Furthermore, **2** functions in both the solid and solution phases, which provides both the handling convenience of the solid phase and the analytical clarity of the solution phase.

The fuel cell was monitored for performance with combinations of **1** or **2** in either or both electrodes and with either catalyst in the solution or solid phase (Table 1). In solution-phase experiments, the electrodes bore conduits that contained solutions of the catalyst, and streams of water-saturated H_2 or O_2 gas were bubbled through. In solid-phase experiments, the NO_3^- counteranion was replaced by $CF_3SO_3^-$ (OTf^-) to yield the corresponding water-insoluble catalyst. This insoluble catalyst was immobilized on carbon cloth and sandwiched between the electrodes and the proton-conducting polymer electrolyte while the saturated gases

[*] Dr. T. Matsumoto, K. Kim, Prof. S. Ogo
Department of Chemistry and Biochemistry
Graduate School of Engineering, Kyushu University
744 Moto-oka, Nishi-ku, Fukuoka 819-0395 (Japan)
E-mail: ogotcm@mail.cstm.kyushu-u.ac.jp
Homepage: http://web.cstm.kyushu-u.ac.jp/ogo/

[**] This work was supported by the World Premier International Research Center Initiative (WPI Program), grants-in-aid: 18065017 (Chemistry of Concerto Catalysis), 19205009 and 23655053, the Global COE Program, "Science for Future Molecular Systems" from the Ministry of Education, Culture, Sports, Science and Technology (MEXT) (Japan), and the Basic Research Programs CREST Type, "Development of the Foundation for Nano-Interface Technology" from JST (Japan).

Supporting information for this article is available on the WWW under http://dx.doi.org/10.1002/anie.201104498.

Table 1: Fuel-cell performance.[a]

Entry	Anode catalyst	State of molecular catalyst	Cathode catalyst	State of molecular catalyst	OCV [V]	Maximum current density [$\mu A\,cm^{-2}$]	Maximum power density [$\mu W\,cm^{-2}$]
1	[**1**](OTf)$_2$	solid	[**1**](OTf)$_2$	solid	0.27	78	11
2	[**2**](OTf)	solid	[**2**](OTf)	solid	0.29	64	11
3	[**1**](OTf)$_2$	solid	Pt	–	0.70	127	54
4	[**2**](OTf)	solid	Pt	–	0.73	112	49
5	Pt	–	[**1**](OTf)$_2$	solid	0.48	2210	288
6	Pt	–	[**2**](OTf)	solid	0.52	2684	373
7	[**1**](NO$_3$)$_2$	solution	[**1**](NO$_3$)$_2$	solution	0.32	17	3.2
8	[**2**](NO$_3$)	solution	[**2**](NO$_3$)	solution	0.29	24	3.4
9	[**1**](NO$_3$)$_2$	solution	Pt	–	0.70	51	24
10	[**2**](NO$_3$)	solution	Pt	–	0.75	68	36
11	Pt	–	[**1**](NO$_3$)$_2$	solution	0.58	1700	186
12	Pt	–	[**2**](NO$_3$)	solution	0.58	1884	231

[a] Electrodes composed of immobilized catalysts [**1**](OTf)$_2$ or [**2**](OTf) on carbon cloth (entries 1–6), dissolved catalysts [**1**](NO$_3$)$_2$ or [**2**](NO$_3$) in the solution phase (entries 7–12), or Pt (entries 3–6 and 9–12). MEA active area: 5 cm^2. Proton-conducting polymer electrolyte: Nafion 212. Carbon black: Cabot Corporation Vulcan XC-72. Carbon cloth: TOYO Corporation EC-CC1-060T. Temperature: 60 °C. Flow rate of water-saturated H_2: 200 mL min^{-1}. Flow rate of water-saturated O_2: 200 mL min^{-1}. Humidity: 100 %.

were passed through the conduits. These systems were studied as part of a polymer electrolyte fuel cell (PEFC) using Nafion 212 or Flemion SH-50 as the proton-conducting polymer electrolyte.

Quantitatively, this cell underperforms in comparison with conventional Pt-based cells, but this might be expected for such a new approach. For instance the **2**–**2** solid-phase fuel cell produced an open-circuit voltage (OCV) of 0.29 V at 60 °C (Figure 2 and Table 1, entry 2), which is somewhat lower than the approximately 1.2 V OCV that can be expected from a Pt-based cell. At the lower cell voltage of 0.29 V, it was able to produce a rather low current density of 64 $\mu A\,cm^{-2}$, corresponding to a maximum power density of 11 $\mu W\,cm^{-2}$.

While these values seem rather low when compared to fully fledged platinum fuel cells, we can expect future designs and developments to significantly improve on this first result. The OCV is dependent on the fundamental thermodynamic properties of the catalyst and is therefore amenable to development in catalyst design. As for the power density, improvements in reaction rate and/or lowering the resistance to catalyst–electrode electron transfer would be expected to bring major benefits.

Over the course of these studies, the solution-phase experiments showed a steady decline in power density compared with the solid-phase experiments. This behavior was the result of small portions of the catalytic solution being flushed out of the conduits of the cell in the exhaust stream. Though this outflow is a result of using solutions in an apparatus designed for solid-state studies, it fortunately provides us with the means to directly, and continually, observe the reaction process—effectively allowing us to sample and observe the solution at any time. We can therefore provide a detailed account of the action of **1** and **2** using evidence based on direct observations from this fuel-cell outflow. Further evidence, obtained by other experimental means, is presented in Tables S1 and S2 in the Supporting Information.

The catalytic cycle of **2** behaving as the anodic catalyst is shown in Scheme 2a, and the full mechanism is shown in Figure S1a in the Supporting Information.[6] In the first step, **2** reacts with H_2 to generate protons and electrons via the low-

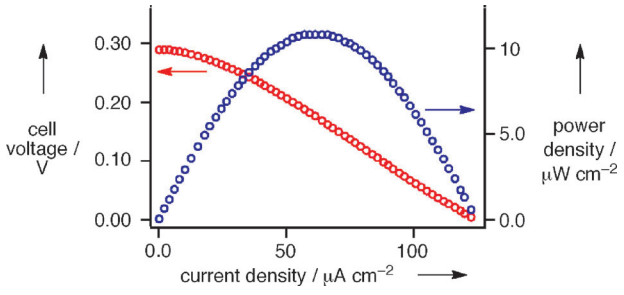

Figure 2. Polarization and power density curve at 60 °C for H_2–O_2 molecular fuel cell. Membrane electrolyte assembly (MEA) active area: 5 cm^2. Anode: Ni^{II} Ru^{II} hydride complex [**2**](OTf) (8.0 μmol). Cathode: Ni^{II} Ru^{II} hydride complex [**2**](OTf) (8.0 μmol). Proton-conducting polymer electrolyte: Nafion 212. Flow rate of water-saturated H_2: 200 mL min^{-1}. Flow rate of water-saturated O_2: 200 mL min^{-1}. Humidity: 100 %. Carbon black: Cabot Corporation Vulcan XC-72. Carbon cloth: TOYO Corporation EC-CC1-060T.

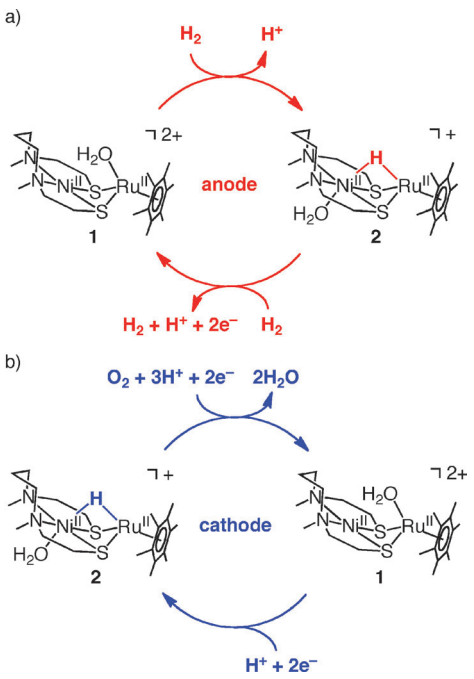

Scheme 2. Proposed mechanisms for a) anodic and b) cathodic reactions based on direct observations from the fuel-cell outflow. Complexes **1** and **2** were isolated from the fuel-cell outflow. The structures of **1** and **2** were determined by X-ray analysis.[6a]

valent Ni^{I} Ru^{I} complex (**3** in Figure S1a in the Supporting Information), producing **1**.[6] Complex **1** then reacts with further H_2 to regenerate the hydride complex **2**. Evidence for this mechanism is described in Table S1, entries 1–4 in the Supporting Information. In the cathodic reaction (Scheme 2b), **2** combines with O_2, three protons, and two electrons to produce **1** via a hydroperoxo intermediate (**4** in Figure S1b in the Supporting Information).[7] By picking up a further proton and two electrons, **1** is reduced back to the hydride complex **2**. This mechanism is supported by observations in Table S2, entries 1 and 2 in the Supporting Information.

We also investigated the reduction of O_2 by a rotating-disk electrode (RDE) at several rotation rates (Figure 3). The currents increase with increasing rotation rate as the rate is varied from 500 to 2500 rpm (Figure 3a). Figure 3b shows a Koutecky–Levich plot of the inverse reduction current at 0 V versus Ag/AgCl as a function of the inverse square root of the rotation rate as the rate is varied from 500 to 2500 rpm. From the slope of the Koutecky-Levich plot, the number of electrons n reducing O_2 was determined. The measured slope yields $n = 4.0$, similar to a reported Cu complex,[3e] thus demonstrating a four-electron reduction of O_2. Additionally, no current attributable to oxidation of H_2O_2 on a ring electrode was observed in rotating ring-disk voltammetry experiments, further indicating that O_2 was reduced to H_2O through a four-electron reduction pathway.

In conclusion, we have applied the novel catalytic action of our NiRu catalyst to both sides of a fully functioning fuel cell. Though the cell currently underperforms in comparison with Pt electrodes and requires the use of Ru, this is only the first step in a radical new approach to fuel-cell catalysis. For instance, we are currently developing the ligand system to allow support on a solid substrate. Hence, by combining the flexibility of the molecular approach with the transparency of solution-phase reactions, we hope to make great steps in developing highly efficient, low-cost catalysts as part of a future hydrogen economy.

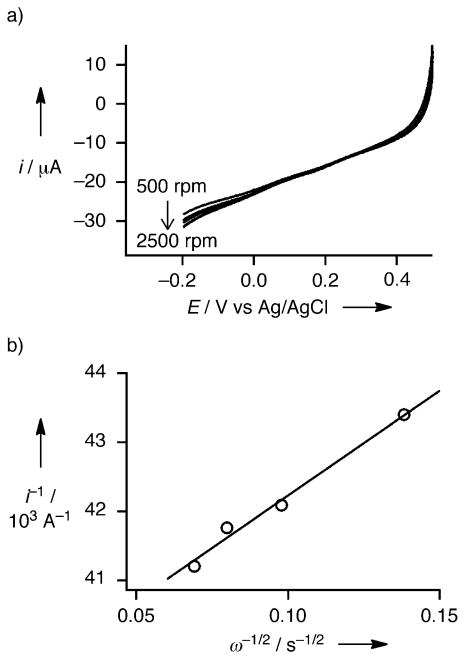

Figure 3. a) Rotating-disk voltammograms for the reduction of O_2 in an O_2-saturated aqueous solution of Ni^{II} Ru^{II} aqua complex [**1**]$(NO_3)_2$ (1.5 mM; working electrode: glassy carbon, counter electrode: Pt, reference electrode: Ag/AgCl, scan rate: 25 $mV s^{-1}$, disk area: 0.07065 cm^2). b) Koutecky–Levich plot of the inverse of the disk current measured at 0 V versus Ag/AgCl as a function of the square root of the inverse of the rotation rate. The fitted line yields $n = 4.0$. The intercept is the inverse of the kinetically limited current $(i_K)^{-1}$. All solutions contained 0.05 M sodium acetate, 0.05 M acetic acid, and 1 M sodium sulfate. The parameters for the Koutecky–Levich plot such as diffusion constant of O_2 (D_{O_2}), concentration of O_2 in O_2-saturated aqueous solution ($[O_2]$), and kinetic viscosity of the solution (ν) were taken from Ref. [3e].

Experimental Section

Membrane electrolyte assembly (MEA) and fuel-cell assembly: In solution-phase experiments, [**1**]$(NO_3)_2$ (5.5 mg, 8.0 μmol) or [**2**](NO_3) (5.0 mg, 8.0 μmol) and carbon black (5.0 mg) were loaded on a waterproof carbon cloth (5 cm^2) to make a gas-diffusion electrode. A piece of a Nafion 212 was sandwiched between two gas-diffusion electrodes and pressed at 25 °C under a pressure of 50 MPa for 30 min. The MEA was assembled in 5 cm^2 fuel-cell hardware. With flow of water-saturated H_2 and O_2 gases, the water-soluble complex **1** or **2** was dissolved in the gas conduits. In solid-phase experiment, complex [**1**]$(NO_3)_2$ (5.5 mg, 8.0 μmol), NaOTf (2.8 mg, 16.2 μmol), and carbon black (5.0 mg) or [**2**](NO_3) (5.0 mg, 8.0 μmol), NaOTf (1.4 mg, 8.1 μmol), and carbon black (5.0 mg) were loaded on a waterproof carbon cloth (5 cm^2) to make a gas-diffusion electrode. A piece of a Nafion 212 was sandwiched between two gas-diffusion electrodes and pressed at 25 °C under a pressure of 50 MPa for 30 min. The MEA was assembled in 5 cm^2 fuel-cell hardware. The NO_3^- counterion of **1** or **2** was replaced by OTf^- to yield a water-insoluble complex, which was held in the gas conduits.

Received: June 29, 2011
Published online: September 12, 2011

Keywords: fuel cells · hydrogen · molecular catalysis · oxygen

[1] a) B. C. H. Steele, A. Heinzel, *Nature* **2001**, *414*, 345–352; b) M. L. Perry, T. F. Fuller, *J. Electrochem. Soc.* **2002**, *149*, S59-S67.

[2] a) K. Asazawa, K. Yamada, H. Tanaka, A. Oka, M. Taniguchi, T. Kobayashi, *Angew. Chem.* **2007**, *119*, 8170–8173; *Angew. Chem. Int. Ed.* **2007**, *46*, 8024–8027; b) R. Bashyam, P. Zelenay, *Nature* **2006**, *443*, 63–66; c) S. Lu, J. Pan, A. Huang, L. Zhuang, J. Lu, *Proc. Natl. Acad. Sci. USA* **2008**, *105*, 20611–20614; d) J. A. Cracknell, K. A. Vincent, F. A. Armstrong, *Chem. Rev.* **2008**, *108*, 2439–2461.

[3] a) Z. M. Heiden, T. B. Rauchfuss, *J. Am. Chem. Soc.* **2007**, *129*, 14303–14310; b) A. Le Goff, V. Artero, B. Jousselme, P. D. Tran, N. Guillet, R. Métayé, A. Fihri, S. Palacin, M. Fontecave, *Science* **2009**, *326*, 1384–1387; c) S. Canaguier, M. Fontecave, V. Artero, *Eur. J. Inorg. Chem.* **2011**, 1094–1099; d) K. Ishiwata, S. Kuwata, T. Ikariya, *J. Am. Chem. Soc.* **2009**, *131*, 5001–5009; e) C. C. L. McCrory, A. Devadoss, X. Ottenwaelder, R. D. Lowe, T. D. P. Stack, C. E. D. Chidsey, *J. Am. Chem. Soc.* **2011**, *133*, 3696–3699.

[4] a) S. Yamazaki, T. Ioroi, Y. Yamada, K. Yasuda, T. Kobayashi, *Angew. Chem.* **2006**, *118*, 3192–3194; *Angew. Chem. Int. Ed.* **2006**, *45*, 3120–3122; b) S. P. Annen et al., *Angew. Chem.* **2010**, *122*, 7387–7391; *Angew. Chem. Int. Ed.* **2010**, *49*, 7229–7233 (see the Supporting Information); c) F. R. Brushett, M. S. Thorum,

N. S. Lioutas, M. S. Naughton, C. Tornow, H.-R. M. Jhong, A. A. Gewirth, P. J. A. Kenis, *J. Am. Chem. Soc.* **2010**, *132*, 12185 – 12187.
[5] S. Ogo, *Jpn. Kokai Tokkyo Koho*, JP 2010059773, **2010**.
[6] a) S. Ogo et al., *Science* **2007**, *316*, 585 – 587 (see the Supporting Information); b) B. Kure, T. Matsumoto, K. Ichikawa, S. Fukuzumi, Y. Higuchi, T. Yagi, S. Ogo, *Dalton Trans.* **2008**, 4747 – 4755; c) T. Matsumoto, B. Kure, S. Ogo, *Chem. Lett.* **2008**, *37*, 970 – 971; d) S. Ogo, *Chem. Commun.* **2009**, 3317 – 3325.
[7] I. Yamanaka, S. Tazawa, T. Murayama, T. Iwasaki, S. Takenaka, *ChemSusChem* **2010**, *3*, 59 – 62.

